On the Probability Density Function of Inter-core Crosstalk Power in Birefringent Homogeneous Multi-core Fibers

Ricardo O. J. Soeiro[1], Tiago M. F. Alves[1] and Adolfo V. T. Cartaxo[1,2]
[1]*Instituto de Telecomunicações, Lisboa 1049-001, Portugal*
[2]*ISCTE - Instituto Universitário de Lisboa, Lisboa 1649-026, Portugal*

Keywords: Coupled Local Mode Theory, Discrete Changes Model, Dual-polarization, Homogeneous Multi-core Fibers, Inter-core Crosstalk.

Abstract: In this paper, the inter-core crosstalk (ICXT) of the polarization directions and the probability density functions (PDFs) of the ICXT power of the polarization directions in weakly coupled birefringent homogeneous multi-core fibers (MCFs) are studied through numerical simulation. The numerical simulator is based on the coupled local mode theory (CLMT), which is a rigorous model that has the downside of requiring long computational times to compute the ICXT field and PDFs of the ICXT power. Conversely, a dual-polarization discrete changes model (DP-DCM) that allows for much faster estimates of the ICXT field is presented. It is shown that, for perfectly homogeneous MCFs, the mean ICXT power distribution between the polarization directions is similar, despite the power distribution at the MCF input, for a mean linear birefringence parameter ranging from 10^{-7} (low birefringence) to 10^{-4} (high birefringence), and for different MCF bending radii. It is also shown that the mean ICXT power estimates obtained with the CLMT and DP-DCM are very similar. Furthermore, using the CLMT, the PDFs of the ICXT power of the polarization directions are shown to be chi-squared distributions with two degrees of freedom, and the PDF of the sum of the ICXT power of the polarizations is shown to follow a chi-squared distribution with four degrees of freedom.

1 INTRODUCTION

Multi-core fibers (MCFs) have been proposed to increase capacity in long haul transmission (Qian et al., 2012), access networks and data centers (Lee et al., 2014). The similar properties of the cores comprising homogeneous MCFs has been reported as an attractive feature for signal transmission (Luís et al., 2016), (Sakaguchi et al., 2013). In particular, with cores with similar properties, similar propagation times of the signals transmitted in each core are obtained, which promotes the use of multi-dimensional spatial modulation formats (Puttnam et al., 2014), shared receiver resources (Feuer et al., 2012) and space-coding techniques (Eriksson et al., 2015). However, the similar properties of the cores also promotes significant crosstalk between them, i.e. inter-core crosstalk (ICXT) (Luís et al., 2016). Significant reduction of the ICXT power can be achieved by designing the MCF appropriately, e.g., by increasing the distance between cores, which has the downside of reducing the core count, or by enveloping the MCF cores in trenches, the so-called trench assisted MCFs (Sakaguchi et al., 2013).

The previously mentioned constraints and compromises led to the proposal of several ICXT estimation models that take into account the parameters of the MCF, e.g. the core radii, distance between cores, fiber bending and twisting, and fiber length (Hayashi et al., 2011), (Macho et al., 2016). The discrete changes model (DCM) proposed in (Hayashi et al., 2011) allows to estimate the ICXT while studying its dependence on the fiber bending, twist and length in a very fast way. In (Hayashi et al., 2011), the ICXT is reported to result mostly from the points along the longitudinal direction of propagation in which the difference between the effective refractive index of the interfering and interfered cores is zero. These points are referred to as phase matching points (PMPs). Meanwhile, other studies were carried to upgrade the DCM, e.g. in (Luís et al., 2016) the dependence of the ICXT on the modulation frequency is included in the DCM, and in (Cartaxo et al., 2016) the ICXT dependence on the difference between the dispersion parameters of the cores is included. In (Soeiro et al., 2017), the DCM is generalized to a dual-polarization

Soeiro, R., Alves, T. and Cartaxo, A.
On the Probability Density Function of Inter-core Crosstalk Power in Birefringent Homogeneous Multi-core Fibers.
DOI: 10.5220/0006542700360042
In *Proceedings of the 6th International Conference on Photonics, Optics and Laser Technology (PHOTOPTICS 2018)*, pages 36-42
ISBN: 978-989-758-286-8

(DP) scheme. The reason why the DCM has been upgraded to included other effects can be attributed to the fast ICXT estimates it provides in comparison with other models. In particular, models that rely on solving the coupled-mode equations numerically are much more computationally demanding, since the number of steps required to solve the coupled-mode equations numerically is much larger than the number of PMPs required to estimate the ICXT with the DCM (Cartaxo and Alves, 2017). In (Macho et al., 2016), the ICXT is estimated with a rigorous coupled local mode theory (CLMT) model while including the effects of core birefringence, bending and twisting. However, the estimates obtained with such model are much more computationally demanding when compared to the DCM, owing to the necessity of solving the CLMT equations numerically with a step-size that can be of the order of the wavelength ($\approx 10^{-6}$ m).

In (Hayashi et al., 2012), it is shown experimentally that the probability density function (PDF) of the total ICXT power, i.e. the PDF of the sum of the ICXT power of the two polarizations, fits quite well a chi-squared distribution with four degrees of freedom. The following assumptions were proposed to explain this distribution: i) the four ICXT field components (the in-phase and quadrature components of the two polarization directions) are uncorrelated and ii) the ICXT power is equally distributed between the polarization directions, and the variances of the in-phase and quadrature components of the ICXT field in the two polarizations are similar.

In this paper, the distribution of the mean ICXT power between the polarization directions at the MCF output is analyzed through numerical simulation with the CLMT model in weakly-coupled birefringent homogeneous MCFs, for different power distributions at the MCF input and for different birefringence parameters. Additionally, the PDFs of the ICXT power of the polarization directions and total ICXT power obtained from the CLMT are studied when the power distribution between the polarization directions at the MCF input is imposed, in order to assess whether the PDFs reported in (Hayashi et al., 2012) are observed under different power distributions between the polarization directions at the MCF input.

2 DISCRETE CHANGES MODEL WITH DUAL-POLARIZATION SCHEME

In this section, the DP-DCM proposed in (Soeiro et al., 2017) is presented. It is considered that, at the input of a two-core MCF, the slowly varying field amplitude of the signal to be transmitted in the interfering core m, $A_m(z=0)$, where z denotes the longitudinal direction of propagation, is distributed between two perpendicular polarization directions, x and y. The power distribution between the directions of polarization x and y is controlled by a variable ζ which takes on a real value between 0 and 1. At the MCF input, the field of each direction of polarization is given by $A_{m,x}(z=0) = A_m(z=0)\cdot\sqrt{\zeta}$ and $A_{m,y}(z=0) = A_m(z=0)\cdot\sqrt{1-\zeta}$. For ICXT analysis, it is assumed that all the power is injected in core m, i.e. $A_n(z=0) = 0$. At the MCF output (z=L, where L is the MCF length), the field amplitudes of the polarization directions of the interfered core n, $A_{n,x}(z=L)$ and $A_{n,y}(z=L)$ are given by (Soeiro et al., 2017):

$$A_{n,x}(z=L) = A_m(0)\cdot[\sqrt{\zeta}\cdot F_{x,x} + \sqrt{1-\zeta}\cdot F_{y,x}] \quad (1)$$

$$A_{n,y}(z=L) = A_m(0)\cdot[\sqrt{1-\zeta}\cdot F_{y,y} + \sqrt{\zeta}\cdot F_{x,y}] \quad (2)$$

where the functions $F_{x,x}$, $F_{x,y}$, $F_{y,x}$ and $F_{y,y}$ model the ICXT from the input of the interfering core m to the output of the interfered core n. In particular, $F_{x,x}$ and $F_{x,y}$ model the ICXT from the polarization x of core m to the polarizations x and y of core n, respectively. The functions $F_{y,x}$ and $F_{y,y}$ model the ICXT from the polarization y of core m to the polarizations x and y of core n, respectively. These functions include the impact of the MCF parameters, e.g. fiber bending and twisting. In general, the functions F are given by (Soeiro et al., 2017):

$$F_{a,b} = \frac{-j}{\sqrt{2}}\cdot e^{-j\overline{\beta}_n L}\cdot\overline{K}'_{nm}\sum_{k=1}^{N} e^{-j(\overline{\beta}_m-\overline{\beta}_n)\cdot z_k} e^{-j\phi_{nm,k}^{(a,b)}} \quad (3)$$

where a and $b \in \{x,y\}$, N is the number of PMPs, $\overline{K}'_{nm}$ is the discrete coupling coefficient obtained from Eq. (28) of (Cartaxo and Alves, 2017) while substituting the inter-core coupling coefficient, κ_{nm}, by the average inter-core coupling coefficient of the polarization directions, $\overline{\kappa}_{nm} = (\kappa_{nm}^{(x)} + \kappa_{nm}^{(y)})/2$. $\overline{\beta}_m$ and $\overline{\beta}_n$ are the average of the propagation constants of the polarization directions in cores m and n, respectively, i.e., $\overline{\beta_m} = (\beta_m^{(x)} + \beta_m^{(y)})/2$ and $\overline{\beta_n} = (\beta_n^{(x)} + \beta_n^{(y)})/2$ (Agrawal, 2001). $\phi_{nm,k}^{(a,b)}$ is a random variable, uniformly distributed between 0 and 2π, that models random variations of the MCF parameters (Hayashi et al., 2011).

The mean ICXT power of the polarization directions x and y are given by $\langle XT_x\rangle = \langle |A_{n,x}(L)|^2/|A_m(0)|^2\rangle$ and $\langle XT_y\rangle = \langle |A_{n,y}(L)|^2/|A_m(0)|^2\rangle$, respectively, where $\langle\cdot\rangle$ is the expected value operator.

The DP-DCM was derived under the conditions that (Soeiro et al., 2017): (i) equal power distribution between the polarization directions is observed at the MCF output, i.e. $\langle XT_x\rangle$=$\langle XT_y\rangle$, despite the value of ζ; (ii) the total mean ICXT power is the same at the MCF output, despite the value of ζ; (iii) the in-phase and quadrature components of $A_{n,x}$ and $A_{n,y}$ are uncorrelated, and one way to ensure this is by imposing that the functions F are uncorrelated between themselves, i.e. $\langle F_{x,x}\cdot F^*_{y,y}\rangle = \langle F_{y,x}\cdot F^*_{x,y}\rangle = \langle F_{x,x}\cdot F^*_{x,y}\rangle = \langle F_{y,x}\cdot F^*_{y,y}\rangle$=0 (Soeiro et al., 2017), where * is the complex conjugate. If conditions (i), (ii) and (iii) are valid, the total mean ICXT power (the sum of the ICXT power of the polarization directions) can be estimated from: $\langle XT\rangle = 2\langle XT_x\rangle = 2\langle XT_y\rangle = 2\langle|F_{a,b}|^2\rangle = N|\overline{K}'_{nm}|^2$ (Soeiro et al., 2017). More details regarding the DP-DCM and its derivation can be found in (Soeiro et al., 2017).

3 NUMERICAL RESULTS AND DISCUSSION

In this section, the numerical simulator based on the CLMT is described and the main parameters of the MCF are presented. The CLMT model is used in subsections 3.1 and 3.2 to analyze the mean ICXT power distribution between the polarization directions and the PDFs of the ICXT power of the polarization directions, respectively.

The numerical CLMT considers weakly coupled linear propagation, modeled by Eq. (17) in (Macho et al., 2016) with the non-linear terms made zero, and a two-core MCF. Each core of the MCF is divided into segments, where in each segment a random birefringence sample, obtained from a Gaussian distribution (Macho et al., 2016) is generated. The mean value of the Gaussian distribution, i.e. the mean linear birefringence, ranges between 10^{-7}, corresponding to a case of low-birefringence, and 10^{-4}, corresponding to a case of high-birefringence (Macho et al., 2016). The standard deviation is 10^{-7}. The refractive index of the cores is 1.4453, and the refractive index of the cladding is 1.4381. The radii of the cores is 4 μm and the distance between cores is 30 μm. The MCF length considered in the numerical results is 200 m and the wavelength is 1550 nm. At the MCF input and at the end of each segment the rotation matrix shown in Eq. (2) of (Wai et al., 1991) is applied to the fields of each core and polarization. The rotation matrix is used in order to ensure random polarization coupling and equal power distribution between the polarization directions. In each segment, the fiber twisting and bending effects are modeled by Eq. 19 of (Macho et al., 2016). In Fig. 1, the total mean ICXT power (sum of the mean ICXT power of the polarization directions) is shown as a function of the number of segments of the cores. The results of Fig. 1 were obtained for a two-core perfectly homogeneous MCF with mean linear birefringence of 2×10^{-7}, a bending radius, $R_b = 0.2$ m, and a fiber twist, $f_T = 0.1$ turns/m. The number of ICXT samples used to compute the mean ICXT power was 500 since it was concluded that this number leads to a large enough sample size to observe convergence of the mean ICXT power estimates, i.e. if more samples were used, similar mean ICXT power estimates would be observed. The number of segments required to observe convergence of the estimated mean ICXT power can be identified from Fig. 1. In particular, it can be concluded that 40 segments are enough for the mean ICXT power estimates to stabilize, i.e., if more segments are considered, the mean ICXT power estimates are similar. Hence, all the results presented from now on will consider 40 segments per core. Table 1 summarizes the parameters used in our study.

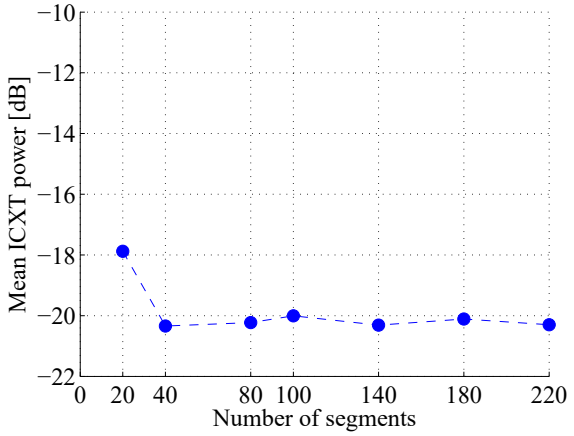

Figure 1: Mean ICXT power as a function of the number of segments for a two-core perfectly homogeneous MCF with mean linear birefringence of 2×10^{-7}, $\zeta = 1$, $R_b = 0.2$ m and $f_T = 0.1$ turns/m.

3.1 Analysis of Mean ICXT Power Distribution between Polarization Directions

In this subsection, the power distribution between the polarization directions is analyzed with the CLMT, for different power distributions between the polarization directions at the MCF input and MCF parameters. The total mean ICXT power, i.e. the sum of the mean ICXT power of the polarizations at the MCF output

Table 1: Main parameters of the 2-core MCF.

Parameter	Value
Refractive index of cladding	1.4381
Refractive index of core n (n_n)	1.4453
Refractive index of core m (n_m)	1.4453
Mean linear birefringence	variable
Distance between cores n and m	30 μm
Core radii	4 μm
Bending radius (R_b)	variable
Fiber twist frequency (f_T)	0.1 turns/m
Fiber length (L)	200 m
Wavelength	1550 nm

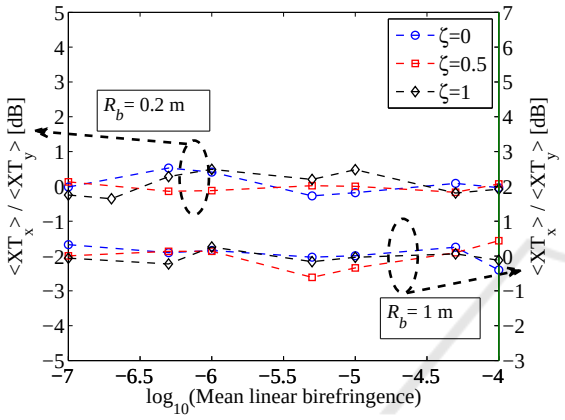

Figure 2: Difference between the mean ICXT power of the polarizations in the interfered core n as a function of the mean linear birefringence for different ζ, $R_b = 0.2$ and 1 m, and $f_T = 0.1$ turns/m.

is also analyzed, and compared to the estimates of the DP-DCM.

In Fig. 2, the difference between the mean ICXT power of the polarizations is shown, in decibel, as a function of the base-10 logarithm of the mean linear birefringence, for different ζ and bending radii. In particular, the results corresponding to the left vertical axis were obtained for $R_b = 0.2$ m and the ones corresponding to the right vertical axis were obtained for $R_b = 1$ m. The remaining parameters employed to obtain the results of Fig. 2 are similar to the ones of Fig. 1. From the results of Fig. 2, it is possible to conclude that similar power distribution between the polarization directions is observed in the interfered core for different ζ and bending radii, as the maximum difference of mean ICXT power between the polarization directions is around 0.5 dB. It should be noted that the difference of mean ICXT power of the polarization directions does not follow a pattern, i.e. in some cases the polarization x has more power than polarization y ($\langle XT_x\rangle/\langle XT_y\rangle > 0$ dB), and in other cases the opposite occurs ($\langle XT_x\rangle/\langle XT_y\rangle < 0$ dB). This observation is important to conclude that the different ζ, mean linear birefringences and bending radii used

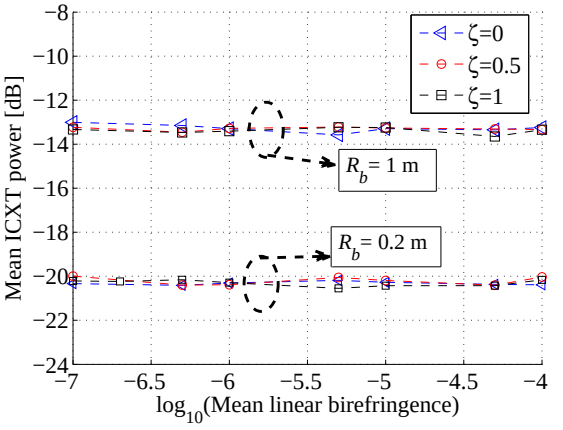

Figure 3: Total mean ICXT power (sum of the mean ICXT power of the x and y polarization directions) as a function of the mean linear birefringence for different ζ, $R_b = 0.2$ and 1 m and $f_T = 0.1$ turns/m.

to obtain the results shown in Fig. 2 do not influence the power distribution between the polarization directions at the MCF output. The fluctuations observed in Fig. 2 are attributed to the randomness of the samples.

Fig. 3 shows the total mean ICXT power (the sum of the mean ICXT power of the polarizations) as a function of the base-10 logarithm of the mean linear birefringence, for different ζ and bending radii. The parameters employed to obtain the results of Fig. 3 are similar to the ones of Fig. 2. From Fig. 3 it is possible to conclude that, for each bending radius, the total mean ICXT power is always around the same value despite ζ and the mean linear birefringence. Furthermore, the total mean ICXT powers shown in Fig. 3 for each bending radius are very similar to the one obtained though the DP-DCM introduced in Section 2, approximately -20.4 dB and -13.0 dB for bending radii of 0.2 m and 1 m, respectively, which shows the accuracy of the DP-DCM. Furthermore, the results obtained with the DP-DCM are much less computationally demanding than the ones obtained with the CLMT. This is attributed to the smaller number of PMPs required to estimate the mean ICXT power when compared to the number of steps required to solve the CLMT equations numerically. In particular, the mean ICXT estimates obtained with the DP-DCM considered 40 PMPs, whereas the step required to solve the CLMT equations numerically was 10^{-4} m. Since a MCF of 200 m is considered, the number of steps used in the CLMT was $200/10^{-4}$=2×10^6, which is more than four orders of magnitude above the number of PMPs considered in the DP-DCM. As a consequence, the results obtained with the CLMT can take several days to obtain, whereas the ones obtained with the DP-DCM only take a few seconds.

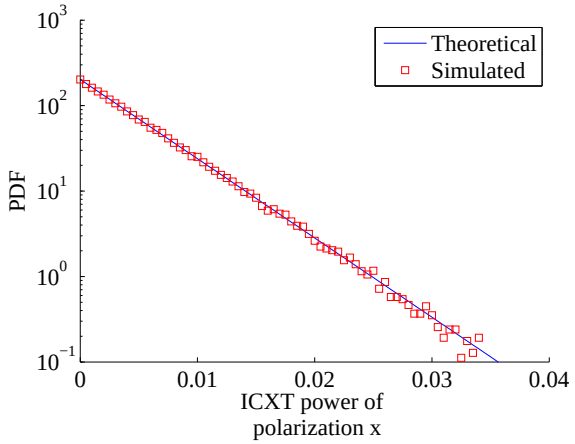

Figure 4: PDF of the ICXT power of polarization x, in logarithmic scale, considering a mean linear birefringence of 2×10^{-7}, $\zeta = 1$, $R_b = 0.2$ m and $f_T = 0.1$ turns/m. The curves obtained through numerical simulation with the CLMT and the corresponding theoretical one are shown.

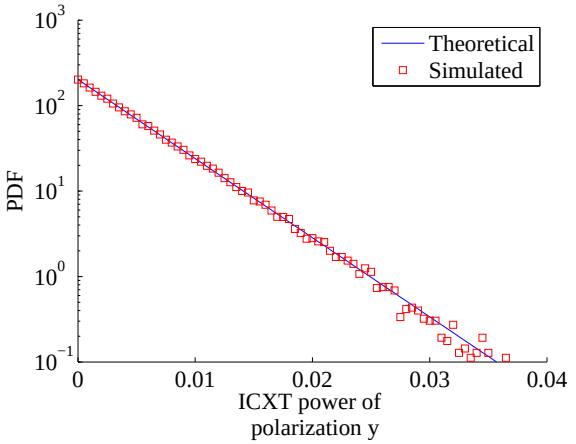

Figure 5: PDF of the ICXT power of polarization y, in logarithmic scale, considering a mean linear birefringence of 2×10^{-7}, $\zeta = 1$, $R_b = 0.2$ m and $f_T = 0.1$ turns/m. The curves obtained through numerical simulation with the CLMT and the corresponding theoretical one are shown.

3.2 Analysis of the PDFs of ICXT Power of the Polarization Directions

In this subsection, the PDFs of ICXT power of the polarization directions are analyzed. The PDF of the total ICXT power, i.e. the PDF of the sum of the ICXT power of the polarization directions is also analyzed.

In Figs. 4 and 5, the PDFs of the ICXT power of polarizations x and y are shown, respectively, obtained for $\zeta = 1$, a mean linear birefringence of 2×10^{-7}, $R_b = 0.2$ m, $f_T = 0.1$ turns/m and using 125000 samples of ICXT power. The y-axis of Figs. 4 and 5 is in logarithmic scale, and the PDFs obtained through numerical simulation with the CLMT are compared with theoretical ones. In Figs. 4 and 5, the theoretical PDFs of the ICXT power in x and y polarizations are chi-squared distributions with two degrees of freedom. The variances of each one of the field components (in-phase and quadrature) of the ICXT field in the x and y polarizations are $\langle XT_x \rangle/2$ and $\langle XT_y \rangle/2$,respectively, where $\langle XT_x \rangle$ and $\langle XT_y \rangle$ are computed from the simulation results. Since $\langle XT_x \rangle \approx \langle XT_y \rangle$, it follows that the variances of each one of the field components are also similar. The agreement between the simulation and theoretical PDFs shown in Figs. 4 and 5 confirms Hayashi's statement that the PDFs of the polarization directions should be chi-squared distributions with two degrees of freedom and similar mean power (Hayashi et al., 2011), even if all the power is injected in the x polarization at the MCF input ($\zeta = 1$). It should be noted that the discrepancy between the theoretical and simulation curves shown in Figs. 4 and 5 is larger for the tail of the PDF. This is a consequence of the limited amount of ICXT power samples obtained through numerical simulation. In particular, the lower the probability density, the less likely we are to obtain the corresponding ICXT power through numerical simulation. Thus, the lower the probability density, the larger the total number of samples we need to consider.

In Fig. 6, the PDF of the sum of the ICXT power of the polarization directions is shown while considering the same parameters of Figs. 4 and 5. The y-axis of Fig. 6 is also in a logarithmic scale, and the comparison between the PDF obtained through numerical simulation with the theoretical one is also shown. In Fig. 6, the theoretical PDF curve of the total ICXT power is obtained from the expression of the chi-squared distribution with four degrees of freedom. The variance of each one of the field components (in-phase and quadrature) of the ICXT field in the x and y polarizations is $(\langle XT_x \rangle + \langle XT_y \rangle)/4$, where $\langle XT_x \rangle$ and $\langle XT_y \rangle$ are obtained from the numerical results. The PDFs shown in Fig. 6 confirm also Hayashi's results (Hayashi et al., 2012), even if all the power is injected in the x polarization at the MCF input ($\zeta = 1$). Similar conclusions were drawn for other power distributions between the polarization directions at the MCF input and bending radii.

4 CONCLUSIONS

The mean ICXT power distribution between the polarization directions and PDFs of the ICXT power of the polarization directions were analyzed in weakly coupled birefringent homogeneous MCFs through nu-

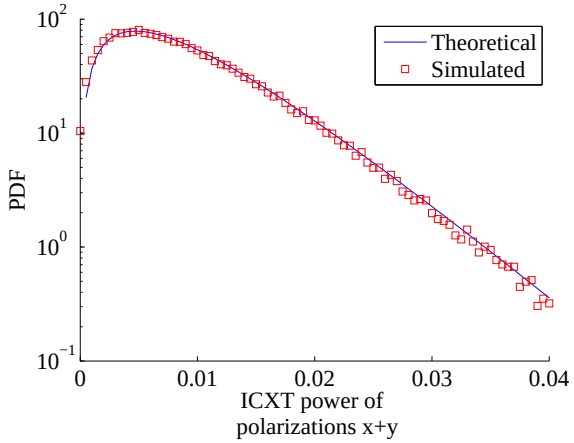

Figure 6: PDF of the total ICXT power of the polarization directions, in logarithmic scale, considering a mean linear birefringence of 2×10^{-7}, $\zeta = 1$, $R_b = 0.2$ m, $f_T = 0.1$ turns/m. The curves obtained through numerical simulation with the CLMT and the corresponding theoretical one are shown.

merical simulation. The numerical simulator based on the CLMT model allowed to conclude that, for perfectly homogeneous MCFs, the mean ICXT power distribution between the polarization directions is similar, despite the power distribution at the MCF input, for a mean linear birefringence parameter ranging from 10^{-7} (low birefringence) to 10^{-4} (high birefringence), and for different MCF bending radii. It was also concluded that the total mean ICXT power estimates obtained with the CLMT and DP-DCM are very similar. Additionally, the PDFs of the ICXT power of the polarization directions obtained with the CLMT were shown to be chi-squared distributions with two degrees of freedom, and the PDF of the sum of the ICXT power of the polarizations was shown to be a chi-squared distribution with four degrees of freedom, showing that Hayashi's results (Hayashi et al., 2012) are valid for different power distributions between the polarization directions at the MCF input.

ACKNOWLEDGEMENTS

This work was supported by Fundação para a Ciência e Tecnologia (FCT), Portugal, under the project AMEN-UID/EEA/50008/2013 of Instituto de Telecomunicações, and the FCT researcher contract IF/01225/2015/CP1310/CT0001.

REFERENCES

Agrawal, G. (2001). *Nonlinear Fiber Optics*. Academic Press, 3rd edition.

Cartaxo, A. V. T. and Alves, T. M. F. (2017). Discrete changes model of inter-core crosstalk of real homogeneous multi-core fibers. *Journal of Lightwave Technology*, 35(12):2398–2408.

Cartaxo, A. V. T., Luís, R. S., Puttnam, B. J., Hayashi, T., Awaji, Y., and Wada, N. (2016). Dispersion impact on the crosstalk amplitude response of homogeneous multi-core fibers. *IEEE Photonics Technology Letters*, 28(17):1858–1861.

Eriksson, T. A., Luís, R. S., Puttnam, B. J., Mendinueta, J. M. D., Andrekson, P. A., Karlsson, M., Awaji, Y., Wada, N., and Agrell, E. (2015). Single parity check-coded 16qam over spatial superchannels in multicore fiber transmission. *Optics Express*, 23(11):14569–14582.

Feuer, M. D., Nelson, L. E., Zhou, X., Woodward, S. L., Isaac, R., Zhu, B., Taunay, T. F., Fishteyn, M., Fini, J. M., and Yan, M. F. (2012). Joint digital signal processing receivers for spatial superchannels. *IEEE Photonics Technology Letters*, 24(21):1957–1960.

Hayashi, T., Taru, T., Shimakawa, O., Sasaki, T., and Sasaoka, E. (2011). Design and fabrication of ultra-low crosstalk and low-loss multi-core fiber. *Optics Express*, 19(17):16576–16592.

Hayashi, T., Taru, T., Shimakawa, O., Sasaki, T., and Sasaoka, E. (2012). Characterization of crosstalk in ultra-low-crosstalk multi-core fiber. *Journal of Lightwave Technology*, 30(4):583–589.

Lee, Y., Tanaka, K., Nomoto, E., Arimoto, H., and Sugawara, T. (2014). Multi-core fiber technology for optical-access and short-range links. In *2014 12th International Conference on Optical Internet 2014 (COIN)*, pages 1–2.

Luís, R. S., Puttnam, B. J., Cartaxo, A. V. T., Klaus, W., Mendinueta, J. M. D., Awaji, Y., Wada, N., Nakanishi, T., Hayashi, T., and Sasaki, T. (2016). Time and modulation frequency dependence of crosstalk in homogeneous multi-core fibers. *Journal of Lightwave Technology*, 34(2):441–447.

Macho, A., García-Meca, C., Fraile-Peláez, F. J., Morant, M., and Llorente, R. (2016). Birefringence effects in multi-core fiber: coupled local-mode theory. *Optics Express*, 24(19):21415–21434.

Puttnam, B. J., Eriksson, T. A., Mendinueta, J.-M. D., Luís, R. S., Awaji, Y., Wada, N., Karlsson, M., and Agrell, E. (2014). Modulation formats for multi-core fiber transmission. *Optics Express*, 22(26):32457–32469.

Qian, D., Ip, E., Huang, M.-F., jun Li, M., Dogariu, A., Zhang, S., Shao, Y., Huang, Y.-K., Zhang, Y., Cheng, X., Tian, Y., Ji, P., Collier, A., Geng, Y., Linares, J., Montero, C., Moreno, V., Prieto, X., and Wang, T. (2012). 1.05pb/s transmission with 109b/s/hz spectral efficiency using hybrid single- and few-mode cores. In *Frontiers in Optics 2012/Laser Science XXVIII*, page FW6C.3. OSA.

Sakaguchi, J., Puttnam, B. J., Klaus, W., Awaji, Y., Wada, N., Kanno, A., Kawanishi, T., Imamura, K., Inaba, H., Mukasa, K., Sugizaki, R., Kobayashi, T., and Watanabe, M. (2013). 305 tb/s space division multiplexed transmission using homogeneous 19-core fiber. *Journal of Lightwave Technology*, 31(4):554–562.

Soeiro, R. O. J., Alves, T. M. F., and Cartaxo, A. V. T. (2017). Dual polarization discrete changes model of inter-core crosstalk in multi-core fibers. *IEEE Photonics Technology Letters*, 29(16):1395–1398.

Wai, P. K. A., Menyuk, C. R., and Chen, H. H. (1991). Stability of solitons in randomly varying birefringent fibers. *Optics Letters*, 16(16):1231–1233.